Prepublished copy

Nature Environment & Pollution Technology

This is a peer-reviewed prepublished version of the paper to be published in Vol. 25, No. 4, December 2026 issue

Original Research Paper

A Hybrid Coagulation–Microfiltration Approach for Industrial Wastewater Pretreatment

Anurag Chavan[1]†, Sanjay Harke[2], Ravindra Gaikwad[3] and Bhavanipant Pande[1]

[1] Department of Environmental Science, School of Basic and Applied Sciences, MGM University, Chh Sambhajinagar, Maharashtra, India
[2] Department of Biotechnology, Institute of Biosciences and Technology, MGM University, Chh Sambhajinagar, Maharashtra, India
[3] Department of Chemical Engineering, Jawaharlal Nehru Engineering College, MGM University, Chh Sambhajinagar, Maharashtra, India
†Corresponding author: Anurag Chavan; anuragschavan@gmail.com

[1] 0009-0008-7036-0083; Anurag Chavan

[2] 0000-0003-1001-0256; Sanjay Harke

[3] 0000-0001-9195-2055; Ravindra Gaikwad

Key Words	Ceramic membrane, Microfiltration, Industrial wastewater, *Moringa oleifera*, Coagulation, CETP pre-treatment, Sustainable wastewater management
DOI	https://doi.org/10.46488/NEPT.2026.v25i04.B4414 (DOI will be active only after the final publication of the paper)
Citation for the Paper	Chavan, A., Harke, S., Gaikwad, R. and Pande, B., 2026. A hybrid coagulation–microfiltration approach for industrial wastewater pretreatment. *Nature Environment and Pollution Technology*, 25(4), B4414. https://doi.org/10.46488/NEPT.2026.v25i04.B4414

ABSTRACT

Common Effluent Treatment Plants (CETPs) frequently receive mixed industrial effluents rich in organic and inorganic pollutants, often exceeding the capacity of conventional biological treatment systems. The present work evaluates the potential of a ceramic microfiltration membrane as a pre-treatment step to improve influent quality prior to CETP processing. Composite wastewater samples from diverse industrial sources were treated by direct membrane filtration and by coagulant-assisted filtration using aluminum sulfate and Moringa oleifera seed powder. An

assembly of commercially available membrane (effective area: 0.0407 m^2) was operated at a transmembrane pressure of 1.0 kg cm^{-2}. The membrane was characterized by FESEM–EDS, XRD, XPS, and porosity analyses to determine its structural and compositional features. Preliminary findings showed appreciable improvement in the physicochemical quality of the treated wastewater, including reduced organic and particulate matter and pH stabilization conducive to biological treatment. The study confirms that ceramic microfiltration, when integrated with chemical and natural coagulants, offers a sustainable and efficient approach to enhance CETP operation and industrial wastewater management.

Introduction

Industrial clusters in emerging economies often generate heterogeneous effluents discharged into shared infrastructures known as Common Effluent Treatment Plants (CETPs). These collective facilities provide economies of scale for small and medium industries but frequently encounter performance limitations when influent wastewater contains excessive organic and inorganic loads that surpass the treatment capacity of conventional biological systems (Padalkar, Hiralal 2018 and Singh et al 2023). Overloading results in lower removal efficiencies, biomass inhibition, excessive sludge generation, and rising operational costs. The situation becomes more complex when the influent comprises mixed industrial wastewater, varying widely in chemical composition and pollutant concentration.

Mixed industrial effluents differ fundamentally from domestic or single-industry wastewater. They typically contain variable concentrations of chemical oxygen demand (COD), biological oxygen demand (BOD), total suspended solids (TSS), total dissolved solids (TDS), heavy metals, salts, and non-biodegradable compounds. Such variability imposes a heavy burden on biological reactors, leading to unstable operation and shock loads that can inhibit microbial activity (Sravan, et al 2024). A field investigation in an Indian CETP reported a marked decline in reliability and pollutant removal efficiency when influent quality deviated from the plant's design range (Ali, et al 2021). This observation underlines the urgent need for robust pre-treatment technologies that can stabilize influent characteristics before biological treatment.

Pre-treatment stages are designed to protect downstream biological units by removing refractory organics, solids, and colloidal matter while improving overall effluent compatibility. Membrane-based separations, especially microfiltration (MF) and ultrafiltration (UF), have attracted attention

as effective methods for the removal of suspended and colloidal pollutants (Othman 2021). In particular, ceramic microfiltration membranes offer distinct advantages over polymeric counterparts due to their chemical inertness, thermal stability, mechanical strength, and longer operational lifetime (Hakami 2020 and Zhang et al 2023). Such membranes can tolerate aggressive conditions found in industrial wastewater streams, making them ideal candidates for CETP pre-treatment. Recent advances demonstrate their growing application in wastewater polishing and hybrid systems, although high capital cost and potential fouling remain constraints (Akash, et al 2024 and Dashtban Kenari 2025).

In parallel, coagulation–flocculation processes remain central to conventional wastewater treatment and have recently evolved toward greener, bio-based alternatives. Natural coagulants derived from plant materials have shown promising results as sustainable substitutes for alum or ferric salts (Ribeiro et al 2019). *Moringa oleifera* seed powder, in particular, has been extensively studied for its coagulation potential; its cationic proteins act as natural polyelectrolytes that neutralize negatively charged colloids, forming settleable flocs (Ndabigengesere et al 1998 and Yamaguchi et al 2021). Studies have shown that *Moringa* seed-based coagulants can reduce turbidity and COD significantly, offering cost-effective and biodegradable treatment options (Oladoja, 2015). Recent evaluations of its performance in real wastewater matrices, including dormitory and domestic effluents, further confirm its effectiveness and practical applicability (Ogunshina et al. 2023). Integration of such bio-coagulants with membrane processes not only enhances overall pollutant removal but also reduces membrane fouling, energy consumption, and sludge toxicity ("Natural Coagulants for Sustainable Wastewater Treatment." *Processes* 13, no. 6 2023).

Hybrid coagulation–membrane systems combine the advantages of both processes: coagulation reduces particle load and fouling on the membrane surface, while the membrane provides physical separation for fine particulates and organic matter (Nouira, et al 2025). The synergy between these two stages enhances filtration performance and yields a stable effluent suitable for biological treatment. For CETPs, which handle diverse industrial effluents, such hybrid pre-treatment represents a practical and sustainable approach to improving influent quality without major infrastructural modification.

In this context, the present work investigates the feasibility of employing an assembly of commercially available ceramic microfiltration membrane as a pre-treatment step prior to CETP

biological processing. Composite wastewater from multiple industrial sources was treated using two configurations: direct membrane filtration and coagulant-assisted membrane filtration utilizing aluminum sulfate and *Moringa oleifera* seed powder. The ceramic membrane was characterized using FESEM–EDS, XRD, XPS, and porosity analysis to relate material properties to observed filtration behavior. This study aims to evaluate the extent to which ceramic microfiltration, combined with natural and conventional coagulants, can reduce organic, particulate, and dissolved loads, thus improving the suitability of mixed industrial wastewater for downstream biological treatment and contributing to sustainable CETP operation.

Although hybrid coagulation–membrane systems have been investigated previously, their application to highly variable composite influent from operating Common Effluent Treatment Plants remains insufficiently explored. The present study advances existing knowledge in four principal ways. First, it evaluates treatment performance using real mixed industrial CETP influent rather than synthetic or single-source wastewater, thereby addressing practical variability and shock-loading conditions. Second, it employs a simultaneous hybrid dosing strategy combining aluminum sulfate and Moringa oleifera extract to deliberately tailor floc characteristics for fouling mitigation rather than solely for turbidity removal. Third, the investigation quantifies fouling reversibility through clean-water flux recovery analysis, providing operational insight into membrane sustainability. Finally, the system is assessed from the perspective of enhancing downstream biological process stability, positioning the membrane unit as a CETP pretreatment stabilizer rather than a polishing step. These aspects collectively define the specific contribution of this work.

2. Materials and Methods

2.1 Collection and Characterization of Composite Wastewater

Composite industrial wastewater was obtained from the influent channel of a Common Effluent Treatment Plant (CETP) serving a mixed industrial cluster composed of textile dyeing, electroplating, food processing, and chemical units. Grab samples were collected during peak discharge hours on three consecutive operating days to capture compositional variability. Samples were stored in acid-washed 20 L HDPE containers, kept at 4 ± 2 °C during transport, and processed within 24 h to minimize changes in chemical characteristics (Federigi *et al.* 2024).

Initial characterization of the wastewater included determination of pH, total dissolved solids (TDS), total suspended solids (TSS), turbidity, chemical oxygen demand (COD), and five-day biological oxygen demand (BOD_5). All measurements followed *Standard Methods for the Examination of Water and Wastewater* (APHA. *Standard Methods for the Examination of Water and Wastewater.* 23rd ed. Washington, DC: American Public Health Association, 2017). Each parameter was determined in triplicate, and average values with standard deviations (SD) were reported to ensure accuracy and reproducibility.

Sampling was intentionally conducted during peak discharge periods to evaluate treatment performance under elevated loading conditions commonly encountered in CETP operations. The reported values therefore reflect representative high-influent operational scenarios rather than long-term seasonal averages. It is acknowledged that industrial influent characteristics may vary seasonally and across full 24-hour operational cycles due to production scheduling, rainfall events, and discharge intermittency. The present dataset captures short-term operational variability but does not encompass extended seasonal fluctuations. Accordingly, the findings should be interpreted within the context of peak-condition performance assessment, and future work will include longer-term multi-season monitoring to strengthen representativeness.

2.2 Coagulants and Preparation of Hybrid Coagulant System

Two coagulant components — aluminum sulfate ($Al_2(SO_4)_3 \cdot 18H_2O$; Merck, India) and *Moringa oleifera* seed powder — were combined to formulate a hybrid coagulant system. Mature *Moringa oleifera* seeds were obtained locally, deshelled, air-dried at ambient temperature, and ground in a stainless-steel mill. The powder was sieved through a 300 µm mesh and stored in airtight containers to prevent moisture absorption (Ofomi et al., 2025). For stock preparation, 10 g of Moringa powder was suspended in 1 L of distilled water, stirred at 150 rpm for 30 min, and left to settle for 1 h. The clear supernatant was decanted and used as the natural coagulant extract (Desta & Bote, 2021)

The combined coagulant system used in this study consisted of aluminum sulfate and *Moringa oleifera* seed extract mixed together in the same solution**. T**he rationale for this combination was to exploit the complementary coagulation mechanisms—charge neutralization by Al^{3+} ions from alum and adsorption–bridging by cationic proteins present in Moringa seeds. The hybrid formulation aimed to enhance floc formation, improve removal efficiency, and reduce the

membrane fouling potential. Based on preliminary jar tests, the optimized doses were 150 mg L^{-1} of alum and 250 mg L^{-1} of Moringa extract, added simultaneously to the wastewater prior to filtration (Kane et al., 2016).

2.2. 1 Coagulant Dose Optimization

Preliminary jar tests were performed using combined alum and Moringa oleifera extract to determine suitable operating doses prior to membrane experiments. Alum concentrations between 50–250 mg L^{-1} and Moringa extract between 100–400 mg L^{-1} were screened in hybrid combinations. Optimization was based on turbidity reduction, floc formation characteristics (size and compactness), settling clarity after 30 min, and residual COD in the supernatant. The selected doses (150 mg L^{-1} alum and 250 mg L^{-1} Moringa extract) provided effective clarification while avoiding excessive sludge formation.

The study was designed to evaluate the hybrid formulation as an integrated pretreatment approach; individual alum-only and Moringa-only systems were not independently optimized within the present scope. Accordingly, quantitative assessment of synergistic interaction was beyond the objectives of this work and is recommended for future investigation.

2.3 Ceramic Membrane Module and Characterization

A commercially available tubular ceramic microfiltration membrane (Membralox®, Pall Corporation, USA) was employed for the study. The membrane consisted of α-alumina with a nominal pore size of 0.2 μm, an effective surface area of 0.0407 m^2, and a length of 250 mm. It was mounted in a stainless-steel cross-flow module equipped with inlet and outlet pressure gauges to monitor operating pressure. Filtration was driven by a variable-speed peristaltic pump (Watson Marlow® 520 series) operated at a constant transmembrane pressure (TMP) of 1.0 kg cm^{-2} and at room temperature (25 ± 2 °C), consistent with typical tubular α-alumina microfiltration setups reported in the literature (Eren and Arslanoğlu 2025).

The physical and surface characteristics of the ceramic membrane were analyzed before experimental runs using Field Emission Scanning Electron Microscopy (FESEM) coupled with Energy-Dispersive X-ray Spectroscopy (EDS) for morphology and elemental composition. Crystalline phases were confirmed through X-ray Diffraction (XRD; Rigaku Ultima IV), while surface elemental states were examined using X-ray Photoelectron Spectroscopy (XPS; Thermo

Scientific ESCALAB Xi⁺). Total porosity was evaluated by the Archimedes water-immersion method, following the protocol described by (Hristov *et al.* 2012).

2.3.1 Porosity Measurement

The total porosity (ε) of the ceramic membrane was determined using the **Archimedes water-immersion method**, following the procedure of (Hristov *et al.* 2012)
The dry membrane sample was weighed (W_1), immersed in deionized water under vacuum for 30 min to ensure complete saturation, and the wet weight (W_2) was recorded after surface wiping. The saturated sample was then suspended in water, and its apparent weight (W_3) was measured using a precision balance. The membrane porosity was calculated using:

$$\varepsilon(\%) = \frac{(W_2 - W_1)}{(W_2 - W_3)} \times 100$$

where W_1, W_2, and W_3 represent the dry, wet, and suspended weights of the membrane, respectively.
All measurements were conducted in triplicate, and mean values ± standard deviation were reported. The obtained porosity (43 ± 2%) was consistent with values typical of mesoporous α-alumina supports.

2.4 Filtration Experiments

a) Direct Membrane Filtration (DMF)

In the direct filtration mode, untreated wastewater was fed to the membrane module without pre-treatment. Each run was carried out for 60 min under a fixed TMP of 1.0 kg cm^{-2}. Permeate was collected at 10-min intervals using a digital balance connected to a data logger to record cumulative mass. The instantaneous permeate flux (J, L m^{-2} h^{-1}) was calculated as:

$$J = \frac{V}{A\,t}$$

where V is the volume of permeate collected (L), A is the effective membrane area (m^2), and t is filtration time (h) (Sanchis-Perucho et al. 2023)

b) Coagulant-Assisted Membrane Filtration (CAMF)

For the coagulant-assisted mode, the hybrid coagulant system (Alum + Moringa) was added directly to the wastewater under rapid mixing at 200 rpm for 2 min, followed by slow stirring at 40 rpm for 20 min. The mixture was allowed to settle for 30 min, and the clarified supernatant was then subjected to membrane filtration under the same conditions as DMF (Singh et al 2023). The synergistic action of aluminum sulfate and Moringa extract was expected to reduce colloidal load, enhance floc density, and mitigate pore-blocking on the ceramic surface (Katalo et al. 2018).

2.5 Membrane Cleaning and Performance Recovery

After each filtration cycle, the membrane module was flushed with deionized water at 1.5 kg cm^{-2} for 10 min to remove reversible fouling layers. A weekly chemical cleaning was carried out using 0.1 M NaOH at 40 °C for 30 min, followed by rinsing until neutral pH was achieved. Clean-water flux (CWF) was measured before and after cleaning to evaluate fouling reversibility and membrane recovery efficiency **(**Ezugbe & Rathilal 2020**).**

2.6 Analytical Determinations and Data Analysis

All influent and permeate samples were analyzed for pH, TSS, TDS, turbidity, COD, and BOD_5 according to APHA (2017) procedures (Standard Methods for the Examination of Water and Wastewater, 23rd ed., American Public Health Association, Washington, DC, 2017). Pollutant removal efficiency was calculated as:

$$\% \text{ Removal} = \frac{C_i - C_f}{C_i} \times 100,$$

where C_i and C_f are the influent and effluent concentrations, respectively. All measurements were performed in triplicate and expressed as mean ± SD. Statistical analysis was conducted using OriginPro 2022b. Data normality was assessed prior to analysis. For normally distributed data, one-way ANOVA was applied. Non-normally distributed data were analyzed using the Kruskal–Wallis test. Flux was analyzed using an independent samples t-test. Statistical significance was accepted at $p < 0.05$

3. Results and Discussion

3.1 Membrane Characterization

The microstructural and compositional characteristics of the alumina ceramic microfiltration membrane were examined to correlate material features with filtration performance.

FESEM–EDS: FESEM imaging (Fig. 1a) revealed a uniform pore structure typical of sintered α-Al_2O_3 supports. EDS elemental mapping (Fig. 1b) confirmed the predominance of aluminum and oxygen, with minor silicon traces from bonding materials. Post-filtration surfaces demonstrated distinct fouling morphology:

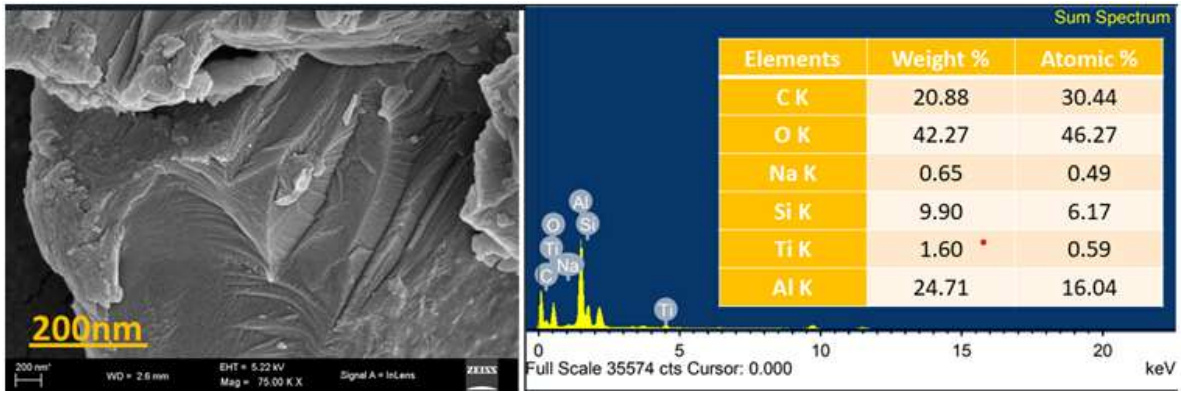

Fig 1 (a) FESEM Micrograph

Fig 1 (b) EDS Spectrum

Figure 1**.** (a) FESEM micrograph of the α-Al_2O_3 support surface showing a uniform, interconnected pore structure at the nanoscale (scale bar: 200 nm).

(b) EDS spectrum and quantitative elemental composition confirming the predominance of Al and O consistent with Al_2O_3, with minor Si, Na, Ti, and C originating from binder residues and surface contaminants.

Following filtration experiments, the membrane surfaces exhibited distinct fouling morphologies, consisting of deposited particulates and surface films that varied depending on feed composition.

XRD: X-ray diffraction analysis (Fig. 2) exhibited sharp peaks corresponding to α-Al_2O_3 at 2θ = 25.5°, 35.1°, 37.8°, 43.4°, 52.6°, 57.5°, 66.5°, and 76.9°, confirming the crystalline integrity of the alumina phase (JCPDS No. 46-1212). No secondary impurity phases were detected.

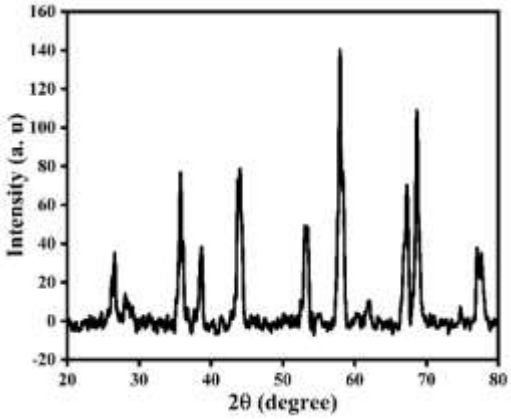

Figure 2: XRD pattern of the commercial α-Al_2O_3 membrane showing characteristic diffraction peaks of the α-alumina phase.

XPS Analysis

X-ray Photoelectron Spectroscopy (XPS) was employed to determine the surface elemental composition and oxidation states of the ceramic membrane (Fig. 3a–f). The survey spectrum confirmed the presence of Al, O, C, Si, Na, and Ti, in agreement with the EDS results.

The high-resolution **C 1s spectrum (Fig. 3a)** exhibits a dominant peak centered at 283.99 eV, characteristic of surface carbon species typically attributed to atmospheric hydrocarbon adsorption. The absence of significant higher-binding-energy components indicates negligible carbonate or oxygenated carbon contamination.

The **Na 1s spectrum (Fig. 3b)** shows a peak at 1071.66 eV, consistent with sodium present in ionic form (Na^+). The relatively weak intensity suggests trace-level sodium, likely originating from precursor materials or processing residues rather than from a distinct sodium-rich phase.

The **Si 2p peak (Fig. 3c)** located at 102.56 eV corresponds to Si^{4+} species in a silicate environment, confirming the presence of silica-based binders or minor secondary phases within the membrane structure.

The **Ti 2p region (Fig. 3d)** displays a Ti $2p_{3/2}$ peak centered at 457.98 eV, indicative of Ti^{4+} in TiO_2. No lower binding energy contributions associated with Ti^{3+} or metallic Ti were observed, suggesting that titanium is present predominantly in its fully oxidized state.

The **O 1s spectrum (Fig. 3e)** presents a strong and symmetric peak at 530.72 eV, characteristic of lattice oxygen (O^{2-}) in metal oxides. The narrow peak profile indicates minimal surface hydroxylation or adsorbed oxygen species.

The **Al 2p spectrum (Fig. 3f)** shows a sharp peak at 73.92 eV, consistent with Al^{3+} in α-Al_2O_3. This binding energy confirms that aluminum exists predominantly in its stable oxide form and constitutes the primary structural framework of the membrane.

Collectively, the high-resolution XPS spectra confirm that the membrane surface is dominated by stable oxide phases (Al–O, Ti–O, and Si–O bonding) with only trace levels of residual sodium and surface carbon. These results further validate the chemical integrity and compositional stability of the α-alumina ceramic matrix.

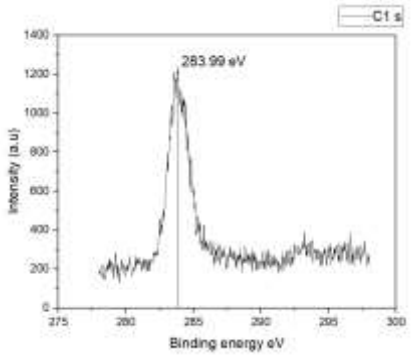

Fig 3a C 1s XPS spectrum with peak at 283.99 eV

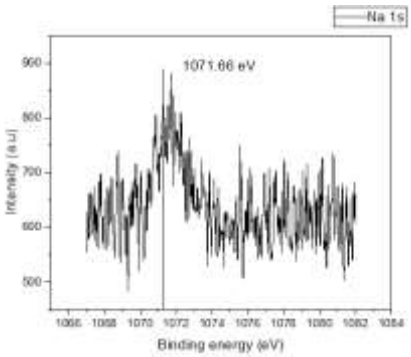

Fig 3b Na 1s XPS spectrum with peak at 1071.66 eV

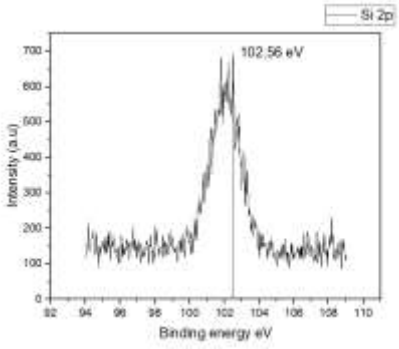

Fig 3c Si 2p XPS spectrum with peak at 102.56 eV.

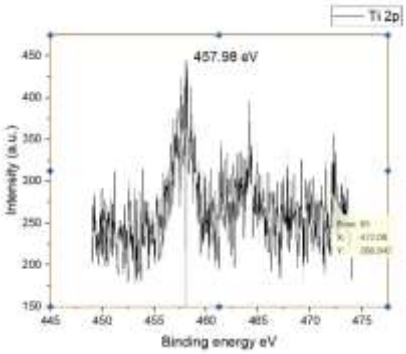

Fig 3d Ti 2p XPS spectrum with peak at 457.98 eV.

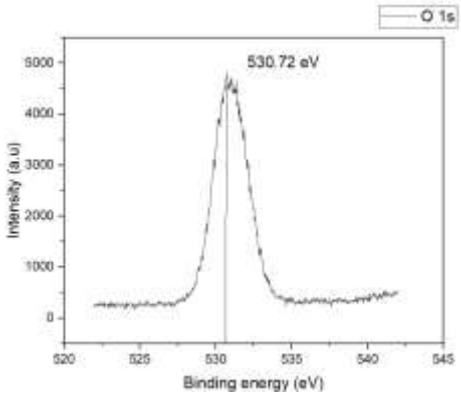

Fig 3e O 1s XPS spectrum with peak at 530.72

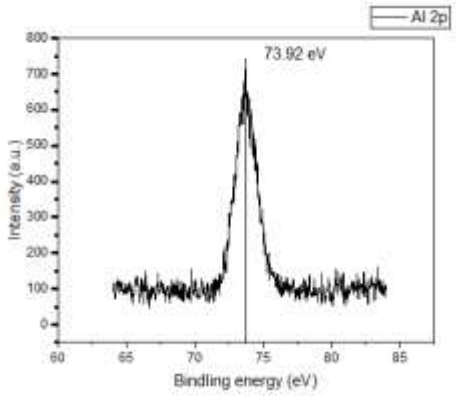

Fig 3f Al 2p XPS spectrum with peak at 73.92 eV.

BET and Porosity: BET analysis yielded a surface area of 90.7 $m^2 g^{-1}$, total pore volume of 0.9469 $cm^3 g^{-1}$, and average pore diameter of ~21 nm. The calculated porosity (Archimedes method) was ~43 ± 2%, characteristic of mesoporous alumina ceramics. The corresponding data are summarized in Table 1.

Parameter	**Method**	**Result**	**Unit**
BET surface area	N_2 adsorption (BET)	90.7	$m^2 g^{-1}$
Langmuir surface area	Langmuir model	97.9	$m^2 g^{-1}$
BJH cumulative surface area (pore > 2 nm)	BJH model	103.0	$m^2 g^{-1}$
Total pore volume (P/Po = 0.9987)	N_2 adsorption	0.9469	$cm^3 g^{-1}$
Average pore diameter	BET	21.0	nm
Micropore surface area	DR model	139.8	$m^2 g^{-1}$
Porosity (Archimedes method)	Water immersion	43 ± 2	%

Table 1 Summary of pore characteristics and surface area measurements of the ceramic microfiltration membrane.

These structural properties, confirmed by complementary XRD and XPS analysis, underpin the observed filtration efficiency and fouling reversibility, as discussed in Sections 3.2 and 3.3.

3.2 Physicochemical Characteristics of Raw Wastewater

The composite industrial effluent collected from the CETP influent exhibited highly variable physicochemical characteristics, as expected for mixed discharges from textile, electroplating, and food-processing units. The raw wastewater was slightly acidic, with pH values ranging between 6.0 and 6.5. Average concentrations of COD (4688 ± 280 mg L^{-1}) and BOD_5 (1523 ± 82 mg L^{-1}) confirmed a high organic load typical of industrial clusters. Elevated TSS (450 ± 28 mg L^{-1}) and TDS (6875 ± 220 mg L^{-1}) reflected substantial solid and dissolved content, while turbidity values near 215 NTU indicated intense coloration and colloidal instability. These results underline the need for pretreatment to improve effluent compatibility with biological processes (APHA. *Standard Methods for the Examination of Water and Wastewater.* 23rd ed. Washington, DC: American Public Health Association, 2017).

3.3 Direct Membrane Filtration (DMF) Performance

Direct ceramic microfiltration of untreated wastewater produced a moderate improvement in water clarity and solids removal but limited organic reduction. The mean turbidity declined from 215 NTU to 59 NTU (approximately 72 %), and TSS decreased by roughly 50 %. COD reduction averaged 22–35 %, consistent with the membrane's ability to retain suspended particles but not dissolved organics. The pH increased slightly to around 6.5 ± 0.2, likely due to partial removal of acidic particulates (Aragonés-Beltrán et al., 2020)**.**

The steady-state flux recorded for DMF averaged 45 L m^{-2} h^{-1} (± 2 L m^{-2} h^{-1}) under a constant transmembrane pressure of 1.0 kg cm^{-2}. A rapid initial decline in flux occurred within the first 15 minutes, after which the rate stabilized, indicating cake-layer formation as the dominant fouling mechanism. Similar trends have been observed in ceramic membranes filtering high-strength industrial effluents (Kapila et al., 2025). Although flux recovery after hydraulic cleaning reached about 87 %, significant reversible fouling persisted, emphasizing the limitation of DMF for untreated complex wastewater.

The moderate COD removal observed in DMF is consistent with the intrinsic pore-size limitation of microfiltration membranes (~0.2 μm), which primarily retain suspended and colloidal matter while allowing dissolved organics to pass through. This explains the limited reduction in dissolved load despite effective turbidity removal.

3.4 Coagulant-Assisted Membrane Filtration (CAMF) Using Combined Alum + *Moringa oleifera*

Pretreatment of the wastewater using a combined coagulant mixture of aluminum sulfate and *Moringa oleifera* seed extract produced a distinct improvement in both water quality and filtration performance. The hybrid coagulant promoted the formation of large, dense flocs through complementary mechanisms—charge neutralization by Al^{3+} ions and adsorption–bridging by cationic Moringa proteins (Kane et al. 2016).

Following CAMF, turbidity was reduced to 17 ± 2 NTU (approximately 92 % removal), and TSS declined to about 9 ± 1 mg L^{-1}, achieving an overall removal efficiency of nearly 80 %. COD and BOD_5 dropped sharply to 855 ± 55 mg L^{-1} and 305 ± 18 mg L^{-1}, corresponding to average reductions of 70–75 % compared to the raw influent. The effluent pH stabilized at 6.8–7.0, a range conducive to downstream biological oxidation (Zielińska & Galik 2017).

The average steady-state flux during CAMF increased to approximately 71 L m^{-2} h^{-1}—around 55 % higher than DMF—demonstrating effective fouling mitigation. The improvement results from decreased colloidal loading and the production of compact, settleable flocs that limit pore blockage (Aragaw and Bogale 2023).

The improved flux behavior under CAMF conditions can be attributed to modification of the feed colloidal matrix prior to membrane contact. Alum promotes charge neutralization of negatively charged particles, while bioactive proteins in Moringa extract facilitate adsorption–bridging. The resulting flocs are larger and less compressible, producing a more permeable cake structure and reducing pore-blocking tendencies.

3.5 Flux behaviour

The variation of permeate flux with time during microfiltration is presented in Fig. 4. Both direct membrane filtration (DMF) and coagulant-assisted microfiltration (CAMF) exhibited an initial sharp decline in flux within the first 10 min, attributed to rapid pore blocking and cake-layer formation by suspended solids and colloidal matter. Thereafter, the flux reached a quasi-steady state due to the establishment of a dynamic filtration layer.

The CAMF system consistently maintained a higher permeate flux (~71 L m^{-2} h^{-1}) compared with DMF (~45 L m^{-2} h^{-1}) throughout the 60-min run, indicating improved fouling control. This enhancement is attributed to the pre-aggregation of colloidal and organic matter by the natural

coagulant (Moringa oleifera) prior to membrane contact, which reduces direct pore deposition and compressibility of the cake layer.

The lower rate of flux decay in CAMF demonstrates the synergistic effect of coagulation and membrane separation, as the coagulant modifies particle size distribution and surface charge, resulting in a more permeable cake structure. Such behaviour aligns with previous reports on hybrid coagulation-membrane systems for industrial wastewater treatment.[4–7]

The observed flux stabilization also indicates partial reversibility of fouling, suggesting that periodic backwashing or hydraulic cleaning can effectively restore flux without significant performance deterioration.

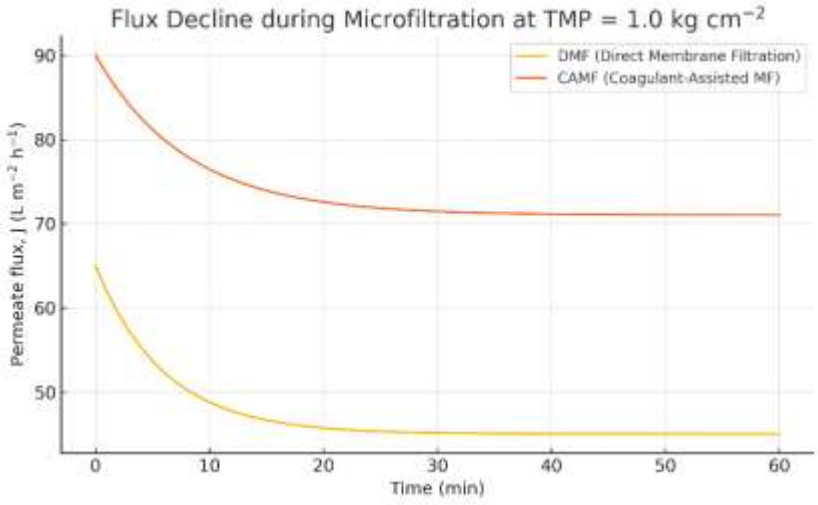

Figure 4: Comparison of flux decline profiles for DMF and CAMF at 1.0 kg cm^{-2}, highlighting slower flux decay and higher steady-state flux under CAMF conditions.

3.6 Comparative Performance and Statistical Evaluation

Table 2 summarizes the results for six representative samples. The overall improvement in pollutant removal and flux enhancement is clearly evident.

Parameter	Raw Effluent (Mean±SD)	DMF (Mean ± SD)	CAMF (Mean ± SD)	Statistic	p-value
pH	6.25 ± 0.18	6.46 ± 0.21	6.80 ± 0.20	13.798[f]	0.000
COD (mg L^{-1})	4688 ± 280	3625 ± 180	855 ± 55	15.158[h]	0.001

BOD_5 (mg L^{-1})	1523 ± 82	1143 ± 46	305 ± 18	15.174[h]	0.001
TSS (mg L^{-1})	450 ± 28	28 ± 2	9 ± 1	15.237[h]	0.000
TDS (mg L^{-1})	6875 ± 220	6560 ± 160	6133 ± 130	12.904[h]	0.002
Turbidity (NTU)	215 ± 8	59 ± 3	17 ± 2	15.205[h]	0.000
Flux (L m^{-2} h^{-1})	–	45 ± 2	71 ± 3	39.51[t]	0.000

Note: [f] F value from one-way ANOVA , [h] H value from Kruskal–Wallis test, [t] t value from independent samples t-test

Table 2. Physicochemical characteristics of raw effluent and effluent treated with DMF and CAMF membranes (mean ± SD). Data normality was assessed prior to analysis. pH was analyzed using one-way ANOVA. COD, BOD_5, TSS, TDS, and turbidity were analyzed using the Kruskal–Wallis test. Flux was analyzed using an independent samples t-test.

The data indicate that CAMF provides nearly double the organic and solids removal of DMF while maintaining significantly higher flux. Statistical analysis confirmed significant differences among raw effluent, DMF, and CAMF samples for COD, BOD_5, TSS, TDS, and turbidity ($p < 0.05$). The marginal change in TDS demonstrates that indicating microfiltration primarily removes suspended and colloidal particles rather than dissolved ions. (Uman et al., 2024).

Flux improvements stem from reduced pore constriction and lower cake resistance, verifying the advantage of pre-coagulation in membrane operations. Similar flux enhancement was reported when combining inorganic and bio-coagulants, attributed to formation of more permeable floc structures (Singh et al 2023). Comparable flux enhancement trends have been reported in other hybrid coagulation–membrane studies, where pre-aggregation of colloids reduced cake resistance and improved hydraulic stability. The present findings align with these observations and support the potential suitability of hybrid pretreatment for treating variable industrial effluents.

3.7 Membrane Fouling and Cleaning Behavior

After each run, the membrane was hydraulically rinsed and chemically cleaned. Clean-water flux recovery reached 95 % after CAMF compared with 87 % after DMF, confirming that hybrid coagulant pretreatment produced a less compact fouling layer and minimized irreversible resistance (Katalo et al. 2018). The combined coagulant also reduced the alum requirement by approximately one-third compared with conventional alum-only systems, contributing to a more sustainable operation.

Overall, these findings validate the effectiveness of integrating hybrid coagulation with ceramic microfiltration for CETP influent pretreatment. The process provides higher organic and solids removal, improved flux stability, and favorable pH conditions, ensuring compatibility with subsequent biological treatment stages.

From an operational perspective, stabilization of pH toward neutrality and reduction of suspended load are particularly beneficial for downstream biological units in CETPs. Lower shock loading and improved influent consistency can reduce biomass inhibition and enhance process reliability under fluctuating industrial discharge conditions.

3.8 Fouling Mechanism Interpretation

Although detailed resistance quantification was not performed, fouling behavior can be interpreted using the classical resistance-in-series concept, where total hydraulic resistance is considered as the sum of intrinsic membrane resistance and fouling resistance. In the present study, fouling development was inferred from flux decline profiles and cleaning recovery behavior.

The sharp initial decrease in permeate flux during the first phase of filtration suggests rapid surface deposition of suspended solids and colloidal matter. Subsequent stabilization of flux indicates formation of a dynamic cake layer governing steady-state resistance rather than continuous internal pore constriction.

Flux recovery after hydraulic rinsing demonstrates that a significant portion of fouling was reversible, attributable to loosely attached cake deposits. The higher recovery observed under coagulant-assisted conditions suggests that pre-aggregation of particles reduced compact pore blocking and limited development of irreversible resistance.

While explicit resistance partitioning (membrane resistance, reversible fouling resistance, and irreversible fouling resistance) would require systematic clean-water flux measurements before and after each filtration cycle, the observed filtration behavior supports cake-dominated fouling under the investigated operating conditions.

Future work involving resistance modeling and pore-blocking kinetics would further strengthen mechanistic understanding at pilot scale.

3.9 Study Limitations

While the hybrid system demonstrated significant improvement in organic and suspended load reduction, dissolved solids removal remained limited, reflecting the inherent constraints of microfilation. Long-term fouling behavior and detailed techno-economic evaluation were beyond the scope of the present study and warrant further investigation prior to large-scale implementation.

3.10 Practical and Scale-Up Considerations

For integration into existing CETP infrastructure, operational and sludge management aspects must be considered. The hybrid coagulation step generates sludge consisting of alum hydroxide flocs combined with aggregated suspended solids and organic matter bridged by Moringa-derived biopolymers. Although quantitative sludge yield was not measured in the present laboratory-scale study, the applied alum dose (150 mg L^{-1}) falls within moderate industrial coagulation ranges and is lower than doses commonly required for highly turbid industrial effluents. Partial substitution of inorganic coagulant with a natural bio-coagulant may reduce inorganic sludge content and associated disposal burden.

The produced sludge would require conventional thickening and dewatering prior to disposal or potential co-processing, consistent with standard CETP sludge management practices. The organic fraction introduced by Moringa extract is biodegradable and may not significantly increase hazardous classification, although detailed sludge characterization remains necessary for full-scale implementation.

From an operational perspective, the microfiltration system operated at 1 kg cm^{-2} (approximately 1 bar), corresponding to low-pressure membrane operation. Under such conditions, typical specific energy consumption for cross-flow microfiltration systems is in the range of 0.2–0.6 kWh m^{-3}, depending on pump efficiency and recovery ratio. These values are considerably lower than those associated with high-pressure nanofiltration or reverse osmosis processes, suggesting favorable energy demand for pretreatment applications.

Chemical consumption under optimized conditions corresponds to 150 mg alum and 250 mg Moringa extract per liter of influent. For a representative CETP treating 1,000 m^3 day^{-1}, this would translate to approximately 150 kg day^{-1} of alum and 250 kg day^{-1} of Moringa extract, subject to influent variability and further optimization.

In terms of footprint, tubular ceramic membrane modules offer compact installation relative to large sedimentation tanks, making retrofitting feasible in space-constrained industrial clusters. However, comprehensive techno-economic assessment and long-term operational trials are necessary to validate cost-effectiveness at full scale.

4. Conclusion

This study evaluated the feasibility of integrating hybrid coagulation (aluminum sulfate combined with *Moringa oleifera* extract) with ceramic microfiltration as a pretreatment strategy for mixed industrial wastewater entering a Common Effluent Treatment Plant (CETP). Under the experimental conditions investigated, the combined approach demonstrated improved reduction of suspended solids, turbidity, and organic load compared with direct membrane filtration alone. Enhanced steady-state flux and higher flux recovery after cleaning indicate reduced fouling propensity when coagulation was applied prior to membrane filtration.

The results suggest that hybrid coagulation–microfiltration can serve as an effective stabilization step for high-strength composite industrial influent under peak loading conditions. However, the findings are based on short-term laboratory-scale experiments using a single membrane configuration and limited temporal sampling. Therefore, the outcomes should be interpreted as proof-of-concept validation rather than full-scale performance confirmation.

While the approach shows potential for improving influent consistency prior to biological treatment, further work is required to assess long-term fouling dynamics, sludge generation characteristics, seasonal variability, and techno-economic feasibility under continuous operation.

Overall, the study provides preliminary evidence supporting the integration of hybrid coagulation with ceramic microfiltration as a pretreatment option for complex industrial wastewater, warranting extended pilot-scale evaluation.

Acknowledgments

The authors gratefully acknowledge MGM University, Chh. Sambhajinagar (MS), for providing the research facilities, laboratory space, and essential operational support that enabled the successful completion of this work.

References

Akash, F.A., Shovon, S.M., Rahman, W. & Monir, M.U. 2024. Advancements in ceramic membrane technology for water and wastewater treatment: A comprehensive exploration of current utilizations and prospective horizons. *Desalination and Water Treatment.* https://www.sciencedirect.com/science/article/pii/S1944398624006192

Ali, M., Almohana, A.I., Alali, A.F., Kamal, M.A., Khursheed, A., Khursheed, A. & Kazmi, A.A. 2021. Common effluent treatment plants monitoring and process augmentation options to conform non-potable reuse. *Frontiers in Environmental Science,* 9:741343. https://doi.org/10.3389/fenvs.2021.741343

American Public Health Association. 2017. *Standard Methods for the Examination of Water and Wastewater.* 23rd ed. American Public Health Association, Washington, DC. https://www.standardmethods.org/?utm_

Aragaw, T.A. & Bogale, F.M. 2023. Role of coagulation/flocculation as a pretreatment option to reduce colloidal/bio-colloidal fouling in tertiary filtration of textile wastewater: A review and future outlooks. *Frontiers in Environmental Science,* 11:1142227. https://doi.org/10.3389/fenvs.2023.1142227

Dashtban Kenari, S.L., Mortazavi, S., Mosadeghsedghi, S., Atallah, C. & Volchek, K. 2025. Advancing ceramic membrane technology for sustainable treatment of mining discharge: Challenges and future directions. *Membranes,* 15(4):112. https://www.mdpi.com/2077-0375/15/4/112?utm_

Desta, W.M. & Bote, M.E. 2021. Wastewater treatment using a natural coagulant (Moringa oleifera seeds): Optimization through response surface methodology. *Heliyon,* 7(11):e08451. https://www.ncbi.nlm.nih.gov/pmc/articles/PMC8637492/

Eren, M.Ş.A. & Arslanoğlu, H. 2025. α-Alumina (α-Al_2O_3) ceramic microfiltration membranes in industrial wastewater treatment: Production, design, filtration behavior and performance. *Ceramics International,* 1–12. https://doi.org/10.1016/j.ceramint.2024.12.454

Ezugbe, E.O. & Rathilal, S. 2020. Membrane technologies in wastewater treatment: A review. *Membranes,* 10(5):89. https://www.ncbi.nlm.nih.gov/pmc/articles/PMC7281250/

Hakami, M.W., Alkhudhiri, A., Al-Batty, S., Zacharof, M.-P., Maddy, J. & Hilal, N. 2020. Ceramic microfiltration membranes in wastewater treatment: Filtration behavior, fouling and prevention. *Membranes,* 10(9):248. https://www.mdpi.com/2077-0375/10/9/248?utm_

Hristov, P., Yoleva, A., Djambazov, St., Chukovska, I. & Dimitrov, D. 2012. Preparation and characterization of porous ceramic membranes for micro-filtration from natural zeolite. *Journal of the University of Chemical Technology and Metallurgy,* 47(4):476–480. https://journal.uctm.edu/node/j2012-4/18-Preslav_476-480.pdf?utm_

Kane, C.K., Bâ, A., Mahamat, S.A.M., Ayessou, N., Mbacké, M.K. & Diop, C.G.M. 2016. Combination of alum and extracted Moringa oleifera bioactive molecules powder for municipal wastewater treatment. *International Journal of Biological and Chemical Sciences,* 10(4):1918–1929. https://agris.fao.org/search/zh/records/6473afc22437ad1e5b938f71?utm_

Kapila, S., Soukup, R.J., Bradley, M.E. & Zydney, A.L. 2025. Flux and fouling behavior during constant pressure sterile filtration of nanoemulsions. *Journal of Membrane Science,* 713:123370. https://doi.org/10.1016/j.memsci.2024.123370

Katalo, R., Okuda, T., Nghiem, L.D. & Fujioka, T. 2018. Moringa oleifera coagulation as pretreatment prior to microfiltration for membrane fouling mitigation. *Environmental Science: Water Research & Technology,* 4:1604–1611. https://doi.org/10.1039/C8EW00186C

Ndabigengesere, A. & Narasiah, K.S. 1998. Quality of water treated by coagulation using Moringa oleifera seeds. *Water Research,* 32(3):781–791. https://www.sciencedirect.com/science/article/abs/pii/S0043135497002959?utm_

Nouira, A., Ben Hamden, M., Sayehi, M. & Bekri-Abbes, I. 2025. Transforming waste to water filters: A mini-review of waste-derived ceramic membranes. *Sustainability,* 3(3):29. https://www.mdpi.com/2813-0391/3/3?utm_

Ofomi, J., Okoye, C., Nnaji, P. & Eze, J. 2025. Testing the performance of powdered Moringa oleifera seed as a natural coagulant for water treatment. *Journal of Environmental Technology & Engineering,* 13(1):xx–xx. https://journals.nipes.org/index.php/jete/article/view/1933

Ogunshina, M.S., Abioye, O.M., Adeniran, K.A. & Olasehinde, D.A. 2023. Moringa oleifera coagulation characteristics in wastewater treatment in a university dormitory. *Nature Environment and Pollution Technology,* 22(2):699–707. https://neptjournal.com/upload-images/%2813%29D-1393.pdf?utm_

Othman, N.H., Alias, N.H., Fuzil, N.S., Marpani, F., Shahruddin, M.Z., Chew, C.M., Ng, K.M.D., Lau, W.J. & Ismail, A.F. 2021. A review on the use of membrane technology systems in water treatment. *Membranes,* 11(1):77. https://pmc.ncbi.nlm.nih.gov/articles/PMC8779680/?utm_

Padalkar, A.V. & Hiralal, V.G. 2018. Common effluent treatment plant (CETP): Reliability and removal efficiencies in an Indian industrial area. *Journal of Environmental Chemical Engineering,* 6(5):6220–6229. https://www.sciencedirect.com/science/article/pii/S1674237018300802?utm_

Ribeiro, J.V.M., Andrade, P.V. & dos Reis, A.G. 2019. Moringa oleifera seed as a natural coagulant to treat low-turbidity water by in-line filtration. *Revista Ambiente & Água,* 14:e2442. https://www.ambi-agua.net/seer/index.php/ambi-agua/article/view/2156?utm_

Sanchis-Perucho, P., Aguado, D., Ferrer, J., Seco, A. & Robles, Á. 2023. Direct membrane filtration of municipal wastewater: Studying the most suitable conditions for minimizing fouling rate in commercial porous membranes at demonstration scale. *Membranes,* 13(1):99. https://www.mdpi.com/2077-0375/13/1/99

Singh, B.J., Chakraborty, A. & Sehgal, R. 2023. A systematic review of industrial wastewater management: Evaluating challenges and enablers. *Science of the Total Environment,* 883:163635. https://www.sciencedirect.com/science/article/pii/S0301479723020182?utm_

Sravan, J.S., Matsakas, L. & Sarkar, O. 2024. Advances in biological wastewater treatment processes: Focus on low-carbon energy and resource recovery in biorefinery context. *Bioengineering,* 11(3):281. https://pmc.ncbi.nlm.nih.gov/articles/PMC10968575/?utm

Uman, A.E., Bair, R.A. & Yeh, D.H. 2024. Direct membrane filtration of wastewater: A comparison between real and synthetic wastewater. *Water,* 16(3):405. https://www.mdpi.com/2073-4441/16/3/405

Yamaguchi, N.U., Cusioli, L.F., Quesada, H.B., Ferreira, M.E.C., Fagundes-Klen, M.R., Salcedo Vieira, A.M.S.S., Gomes, R.G., Vieira, M.F. & Bergamasco, R. 2021. A review of Moringa oleifera seeds in water treatment: Trends and future challenges. *Process Safety and Environmental Protection,*147:405–420. https://www.sciencedirect.com/science/article/abs/pii/S0957582020317626?utm_

Zhang, Y., Tan, Y., Sun, R. & Zhang, W. 2023. Preparation of ceramic membranes and their application in wastewater and water treatment. *Water,* 15(19):3344. https://www.mdpi.com/2073-4441/15/19/3344?utm_

Zielińska, M. & Galik, M. 2017. Use of ceramic membranes in a membrane filtration supported by coagulation for the treatment of dairy wastewater. *Water, Air, & Soil Pollution,* 228:173. https://link.springer.com/article/10.1007/s11270-017-3365-x